DOI 10.1007/s10778-022-01166-x
International Applied Mechanics, Vol. 58, No. 4, July, 2022

DYNAMICS OF SANDWICH CONICAL SHELLS WITH A DISCRETELY INHOMOGENEOUS CORE UNDER NONSTATIONARY LOADING

P. Z. Lugovyi[1*], V. V. Gaidaichuk[2], S. P. Orlenko[1], and K. E. Kontenko[2]**

The dynamics of sandwich conical shells under nonstationary loading is studied. The equations of motion of sandwich conical shells with a discrete symmetric lightweight ribbed core under axisymmetric impulsive loading are derived. In analyzing elements of an elastic shell, the Timoshenko theory of shells and rods is combined with independent static and kinematic hypotheses for each layer. The load-bearing layers in non-symmetric shells are made of dissimilar materials. The equation of motion for a non-symmetric sandwich conical shell with a discretely inhomogeneous core is derived using the Hamilton–Ostrogradsky variational principle. The numerical results on the vibrations of a sandwich elastic shell are obtained using the finite-element method. The influence of the physical and mechanical parameters of symmetric and non-symmetric layers on the stress–strain state of shells under the axisymmetric internal impulsive loading is studied. New mechanical effects are established.

Keywords: dynamics, symmetric and non-symmetric sandwich conical shells, discrete symmetric lightweight core, reinforcing ribs, nonstationary loading, stress–strain state, mechanical effects

Introduction. Layered conical shells are widely used in aircraft engineering, rocket and missile engineering, shipbuilding, and many other fields. The strength and weight requirements and service conditions become more and more severe. The necessity of meeting contradictory requirements leads to the idea of designing multilayer structures wherein each layer performs either just one function or, better, several functions. In this case, the layers may differ in both thickness and physical and mechanical characteristics, which means that the sandwich structure is essentially inhomogeneous.

In what follows, we will consider conical symmetric and non-symmetric sandwich shells of revolution with inhomogeneous lightweight core and discrete-symmetric reinforcement ribs aligned with the lines of principal curvatures and connecting the load-bearing layers. The shells are under forced dynamic loading. The ribs are much smaller than the distance between them. Using cores made of lightweight materials makes it possible to substantially increase the bending stiffness of the structure while moderately increasing its weight. The theory of layered shells in combination with independent hypotheses for each layer would be appropriate for use in this case [12]. Thought this increases the total order of the equations, it becomes possible to analyze the dynamic behavior of a sandwich structure under forced dynamic loading. The paper [8] was among the first to study the dynamics of sandwich conical shells with discrete inhomogeneous core. The publications [6, 9, 10] were the first to analyze the dynamics of sandwich conical shells with a discrete inhomogeneous core under non-stationary loading. The vibrations of sandwich cylindrical shells with a discrete symmetric lightweight core and reinforcement ribs were analyzed in [3, 7, 11, 19, 21–23].

In solving the problem stated, we will use the theory of shells and rods based on the Timoshenko shear model. To derive the equations of vibration of a sandwich shell inhomogeneous across the thickness, we will use the Hamilton–Ostrogradsky variational principle. The dynamics of sandwich conical shells with discrete symmetric lightweight core and reinforcement ribs

[1]S. P. Timoshenko Institute of Mechanics, National Academy of Sciences of Ukraine, 3 Nesterova St., Kyiv, Ukraine, 03057; *e-mail: plugovyy@inmech.kiev.ua. [2]Kyiv National University of Construction and Architecture, 31 Povitroflotskyi Av., Kyiv, Ukraine; **e-mail: viktor_gaydaychuk@ukr.net. Translated from Prykladna Mekhanika, Vol. 58, No. 4, pp. 45–58, July–Augus 2022. Original article submitted July 19, 2021.

will be numerically simulated using the finite-element method. We will present the numerical results for specific problems and point out new mechanical effects.

1. Problem Statement. Basic Equations. A discrete symmetric elastic conical-type structure inhomogeneous across the thickness is a structure composed of inner and outer smooth conical shells (inside and outside load-bearing layers) with certain thicknesses and radiuses. Assume that the middle lines of the shells are parallel, i.e., the cone angle α is the same. A sandwich conical shell with a lightweight core reinforced with discrete ribs is an elastic structure composed of inside (index "1") and outside (index "2") load-bearing layers, lightweight core (index t), and discrete ribs (index j) perfectly bonded to the load-bearing layers. The shell of total constant thickness h has a smooth mid-surface described by orthogonal coordinates s, z. When $z = 0$, the coordinate line s on the mid-surface coincides with the generatrix. The coordinate line z is straight and orthogonal to the mid-surface. Let z be positive if the point lies on the side of the convex part of the mid-surface. Considering the axisymmetric vibrations of conical shells, the coordinate system s, t is used usually, with the coordinate s reckoned from the cone vertex. If the shell is truncated, it is more convenient to use the coordinate s reckoned from the edge of the shell of radius R_0. In this case, the current radius of the conical shell is determined as

$$R_s = R_0 + s\cdot\sin\alpha,$$

where α is the cone angle. The coefficients of the first quadratic form and the curvatures of the coordinate surface of the conical shell are defined by $A_1 = 1, A_2 = R_s, k_1 = 0, k_2 = \cos\alpha / R_s$. The shells are rigidly coupled by discrete ribs and a lightweight core. The strain state mode of the inside and outside load-bearing layers can be expressed in terms of the components of the generalized displacement vector $\overline{U}_1 = (u_s^1, u_3^1, \varphi_1^1)^T$ and $\overline{U}_2 = (u_s^2, u_3^2, \varphi_1^2)^T$ [14]. The displacements fields for the lightweight ribbed core are defined by the generalized displacement vector $\overline{U}_t = (u_s^t, u_3^t, \varphi_1^t)^T$ in accordance with the model from [15]. The strain state of the reinforcing rib directed along the circumferential coordinate is defined by the generalized displacement vector $\overline{U}_J = (u_1^j, u_3^j, \varphi_1^j)^T$.

According to the theory of shear strain in shells [14], the displacements u_1^i and u_3^i in the load-bearing layers in the direction s (longitudinal), z (thickness), and t (time) are expressed as follows if linear displacements are small:

$$u_1^i(s, z, t) = u_0^i(s, t) + z_i\varphi_1^i(s, t),$$

$$u_3^i(s, z, t) = u_{03}^i(s, t) \qquad (i = 1, 2), \tag{1.1}$$

where φ_1^i is the angle between the normal and the mid-surface of the load-bearing layers.

The kinematic equations for the load-bearing layers and the jth rib take the form

$$\varepsilon_{11} = \frac{\partial u_1}{\partial s_1}, \quad \varepsilon_{22} = \frac{1}{A_2}\frac{\partial A_2}{\partial s_1}u_1 + k_2 u_3, \quad \varepsilon_{13} = \varphi_1 + \frac{\partial u_3}{\partial s_1},$$

$$\kappa_{11} = \frac{\partial \varphi_1}{\partial s_1}, \quad \kappa_{22} = \frac{1}{A_2}\frac{\partial A_2}{\partial s_1}\varphi_1, \quad \varepsilon_{22j} = \frac{u_{3j}}{R_j}. \tag{1.2}$$

Since the reinforcement ribs are assumed to be perfectly bonded to the conical load-bearing layers, the interface conditions between the centers of gravity of the ribs and the load-bearing layers are as follows [17]:

$$u_1^j = u_1^{jk}(s_j) \mp \frac{H_j}{2}\varphi_1^{jk}(s_j),$$

$$u_3^j = u_3^{jk}(s_j), \quad \varphi_1^j = \varphi_1^{jk}(s_j) \quad (k = 1, 2), \tag{1.3}$$

where s_j is the coordinate of the line of the projections of the centers of gravity of the cross-sections of the jth rib onto the mid-surface of the load-bearing layer; h_i $(i = 1, 2)$ is the thickness of the spherical load-bearing layers; $H_j / 2$ is the distance from the axis of the jth rib to the surface of the smooth shells; $h_t = H_j$ is the thickness of the lightweight core.

According to [15], the displacements of the lightweight core are expressed by

$$u_1^t(s, z, t) = \left(1 + \frac{z_t}{R_t}\right) u_0^t(s, t) + z_t u_1^t(s, t),$$

$$u_3^t(s, z, t) = u_{03}^t(s, t). \tag{1.4}$$

The kinematic equations for the lightweight core in the case of small strains are as follows:

$$\varepsilon_{11}^t = \frac{\partial u_0^t}{\partial s} + z\frac{\partial u_1^t}{\partial s}, \qquad \varepsilon_{22}^t = \frac{u_{03}^t}{R_{st} + z_t},$$

$$2\varepsilon_{13}^t = \frac{\partial u_{03}^t}{\partial s} + u_1^t, \qquad \kappa_{11}^t = \frac{\partial u_1^t}{\partial s}. \tag{1.5}$$

The compatibility conditions (perfect bonding between the core and the load-bearing layers without separation and slippage) have the following form [16]:

$$u_1^t(z = z_t^1) = u_0^i + \frac{1}{2}(-1)^k h_i \varphi_1^i, \qquad u_{03}^t = u_{03}^i, \qquad \begin{cases} \text{for } i = 1 \rightarrow \left(k = 0;\ z_t^1 = -\dfrac{h_t}{2}\right); \\ \text{for } i = 2 \rightarrow \left(k = 1;\ z_t^2 = \dfrac{h_t}{2}\right). \end{cases} \tag{1.6}$$

Using the expressions for the displacement field of the load-bearing layers (1.2) and lightweight core (1.4), we simplify the compatibility conditions (1.6):

$$u_0^t = \frac{u_0^1 + u_0^2}{2} - \frac{1}{4}(h_2\varphi_1^2 - h_1\varphi_1^1),$$

$$u_1^t = \frac{u_0^1 - u_0^2}{h_t} - \frac{1}{2h_t}(h_2\varphi_1^2 + h_1\varphi_1^1),$$

$$u_{03}^t = \frac{1}{2}(u_{03}^1 + u_{03}^2). \tag{1.7}$$

The equations of motion for the load-bearing layers and the lightweight core are derived from the Hamilton–Ostrogradsky variational stationarity principle:

$$\delta\int_{t_1}^{t_2}(K - \Pi + A)dt = 0, \tag{1.8}$$

where Π is the total potential energy of the elastic system; K is the total kinetic energy of the elastic system; A is the work done by the external forces; t_1 and t_2 are fixed instants of time.

In deriving the equations of vibration of sandwich shells with lightweight core, the displacement components of the load-bearing layers, reinforcement ribs, and the lightweight core must be varied independently. The variations of the total potential and kinetic energy of these components are

$$\delta\Pi = \delta\sum_{i=1}^{2}\Pi^i + \delta\sum_{j=1}^{J}\Pi^j + \delta\sum_{S_t}\Pi^t,$$

$$\delta K = \delta\sum_{i=1}^{2}K^i + \delta\sum_{j=1}^{J}K^j + \delta\sum_{S_t}K^t, \tag{1.9}$$

where

$$\delta\Pi^i = \int_{S_i}\left[\int_{-h/2}^{h/2}(T_{11}^i\delta\varepsilon_{11}^i + T_{22}^i\delta\varepsilon_{22}^i + T_{13}^i\delta\varepsilon_{13}^i + M_{11}^i\delta\kappa_{11}^i + M_{22}^i\delta\kappa_{22}^i)dz_i\right]dS_i, \tag{1.10}$$

$$\delta\Pi^t = \int_{S_t}\left[\int_{-h_t/2}^{h_t/2}(T_{11}^t\delta\varepsilon_{11}^t + T_{13}^t\delta\varepsilon_{13}^t + M_{11}^t\delta\kappa_{11}^t)dz_t\right]dS_t, \tag{1.11}$$

$$\delta\Pi^j = \int_{L_J}(T_{11j}\delta\varepsilon_{11j} + T_{13j}\delta\varepsilon_{13j} + M_{11j}\delta\kappa_{11j})dL_J, \tag{1.12}$$

$$\delta K^i = \int_{S_i}\left\{\int_{-h_i/2}^{h_i/2}\left[\rho_i h_i\left(\frac{\partial^2 u_0^i}{\partial t^2}\delta u_0^i + \frac{\partial^2 u_{03}^i}{\partial t^2}\delta u_{03}^i\right) + \rho_i\frac{h_i^3}{12}\left(\frac{\partial^2\varphi_1^i}{\partial t^2}\delta\varphi_1^i\right)\right]dz_i\right\}dS_i, \tag{1.13}$$

$$\delta K^t = \int_{S_t}\left[\int_{-h_t/2}^{h_t/2}\rho_t h_t\left(\frac{\partial^2 u_0^t}{\partial t^2}\delta u_0^t + \frac{\partial^2 u_1^t}{\partial t^2}\delta u_1^t + \frac{h_t^2}{12}\frac{\partial^2 u_{03}^t}{\partial t^2}\delta u_{03}^t\right)dz_t\right]dS_t, \tag{1.14}$$

$$\delta K^j = \int_{L_j}\left[\rho_j F^j\left(\frac{\partial^2 u_1^j}{\partial t^2}\delta u_1^j + \frac{\partial^2 u_3^j}{\partial t^2}\delta u_3^j\right) + \rho_j\left(I_{tw}^j\frac{\partial^2\varphi_1^j}{\partial t^2}\delta\varphi_1^j\right)\right]dL_j, \tag{1.15}$$

where F^j and I_{tw}^j are the geometric characteristics of the cross-sections of the reinforcement ribs; ρ_j is the specific weight of the rib material; ρ_i $(i=1,2)$ and ρ_t are the specific weights of the materials of the load-bearing layers and core, respectively.

The shell being considered is acted upon by internal axisymmetric distributed nonstationary normal loads $P_1(s,t)$, where s and t are the space and time coordinates.

Note that in calculating the potential and kinetic energy for the core, the integrals in the expressions for $\delta\Pi^t$ and δK^t are evaluated over the volume increased by the volume of the ribs. However, this fact hardly influences the error of the shell theory because the volume of ribs in sandwich shells is less than 5% of the core volume.

In deriving the equations of vibration of sandwich shells with lightweight core, the displacement components of the load-bearing layers, reinforcement ribs, and the core are varied.

Performing standard transformations in (1.8) and using (1.9)–(1.15), we arrive at two systems of nine-order hyperbolic equations for an asymmetric sandwich conical shells with a lightweight core reinforced with discrete ribs under axisymmetric impulsive loading and boundary conditions:

$$\frac{1}{A_2^i}\frac{\partial}{\partial s_i}(A_2^i T_{11}^i) - \frac{1}{A_2^i}\frac{\partial}{\partial s_i}(A_2^i T_{22}^i) - \frac{1}{R_t}T_{13}^t = \left(\rho_i h_i + \frac{\rho_t h_t}{3}\right)\frac{\partial^2 u_0^i}{\partial t^2},$$

$$\frac{1}{A_2^i}\frac{\partial}{\partial s_i}(A_2^i M_{11}^i) - \frac{1}{A_2^i}\frac{\partial}{\partial s_i}(A_2^i M_{22}^i) - T_{13}^i - T_{13}^t = \rho_i\frac{h_i^3}{12}\frac{\partial^2\varphi_1^i}{\partial t^2},$$

$$\frac{1}{A_2^i}\frac{\partial}{\partial s_i}(A_2^i T_{13}^i) - k_2 T_{22}^i + \frac{1}{h_t}T_{13}^t - \left(1 \pm \frac{h_i}{2R_{1s}}\right)P_1 = \rho_i h_i\frac{\partial^2 u_{03}^i}{\partial t^2} \quad (i=1,2),$$

$$\frac{\partial T_{11}^t}{\partial x} + \frac{1}{R_t}N_{13}^t = \rho_t h_t\frac{\partial^2 u_0^t}{\partial t^2}, \quad \frac{\partial T_{13}^t}{\partial x} = \rho_t h_t\frac{\partial^2 w_0^t}{\partial t^2}, \quad \frac{\partial M_{11}^t}{\partial x} - T_{13}^t = \rho_t\frac{h_t^3}{12}\frac{\partial^2 u_1^t}{\partial t^2},$$

$$[T_{11}^{i\pm}]_j = \rho_j F_j \frac{\partial^2 u_{1j}}{\partial t^2}, \quad [T_{13}^{i\pm}]_j = \rho_j F_j \frac{\partial^2 u_{3j}}{\partial t^2}, \quad [M_{11}^{i\pm}]_j = \rho_j I_{twj} \frac{\partial^2 \varphi_{1j}}{\partial t^2}, \tag{1.16}$$

where $[T_{11}^{i\pm}]_j, [T_{13}^{i\pm}]_j$, and $[M_{11}^{i\pm}]_j$ on the discontinuity lines are the forces and moments exerted by the load-bearing layers on the jth rib.

For asymmetric sandwich shells, the system of equations (1.16) is decomposed because of not only the discontinuity between the ribs and load-bearing layers, but also the dissimilarity of the materials of the load-bearing layers.

The forces/ moments and the strains in the load-bearing layers and reinforcement ribs are related as follows:

$$T_{11}^i = B_{11}^i(\varepsilon_{11}^i + v_2^i \varepsilon_{22}^i), \quad T_{22}^i = B_{22}^i(\varepsilon_{22}^i + v_1^i \varepsilon_{11}^i), \quad T_{13}^i = k^2 G_{13}^i \varepsilon_{13}^i,$$

$$M_{11}^i = D_{11}^i \kappa_{11}^i, \quad M_{22}^i = D_{22}^i \kappa_{22}^i, \quad T_{22j} = B_{22j}\varepsilon_{22j}, \tag{1.17}$$

where E_i, G_{13}^i, v_i are the physical and mechanical parameters of the load-bearing layers; k^2 is the integral coefficient of transverse shear in the Timoshenko shell theory; E_j and F_j are the elastic modulus of the material and the cross-sectional area of the jth rib, respectively.

The forces and moments for the core can be expressed as

$$T_{11}^t = \int_{-h_t/2}^{h_t/2} \left(1 + \frac{z_t}{R_t}\right) \sigma_{11}^t dz_t,$$

$$M_{11}^t = \int_{-h_t/2}^{h_t/2} z_t \left(1 + \frac{z_t}{R_t}\right) \sigma_{11}^t dz_t,$$

$$T_{13}^t = \int_{-h_t/2}^{h_t/2} \left(1 + \frac{z_t}{R_t}\right) \sigma_{13}^t dz_t. \tag{1.18}$$

The equations of vibration (1.16) are supplemented with boundary and initial conditions.

2. Numerical Results. We have solved the problem of the dynamic deformation of a sandwich conical shell with clamped ends under internal distributed loading $P_1(s, t)$. The boundary conditions for the load-bearing layers at $s = s_0$ and $s = s_N$ are

$$u_1^i = u_3^i = \varphi_1^i = 0 \qquad (i = 1, 2). \tag{2.1}$$

The initial conditions for the load-bearing layers at $t = 0$ are zero:

$$u_1^i = u_3^i = \varphi_1^i = 0, \qquad \frac{\partial u_1^i}{\partial t} = \frac{\partial u_3^i}{\partial t} = \frac{\partial \varphi_1^i}{\partial t} = 0 \qquad (i = 1, 2). \tag{2.2}$$

A nonstationary impulse load is given by

$$P_3 = A \sin \frac{\pi t}{T} [\eta(t) - \eta(t - T)], \tag{2.3}$$

where $\eta(t)$ is the Heaviside function.

The input data for the three-layer structure: $A = 10^6$ Pa, $T = 50 \cdot 10^{-6}$ sec; $E_1^1 = E_1^2 = E_j = 7 \cdot 10^{10}$ Pa, $\rho_1 = \rho_2 = \rho_j = 2.7 \cdot 10^3$ kg/m^3, $\nu_1^1 = \nu_1^2 = \nu_j = 0.3$, $R_0 = 0.3$ m, $R_0 / h_1 = 30$, $h_1 = h_2 = h_j = 0.01$ m, $H_J = 2h_1$, $\alpha = \pi / 12 = 15°$, $F_j = 2 \cdot 10^{-4}$ m^2. There is no lightweight core.

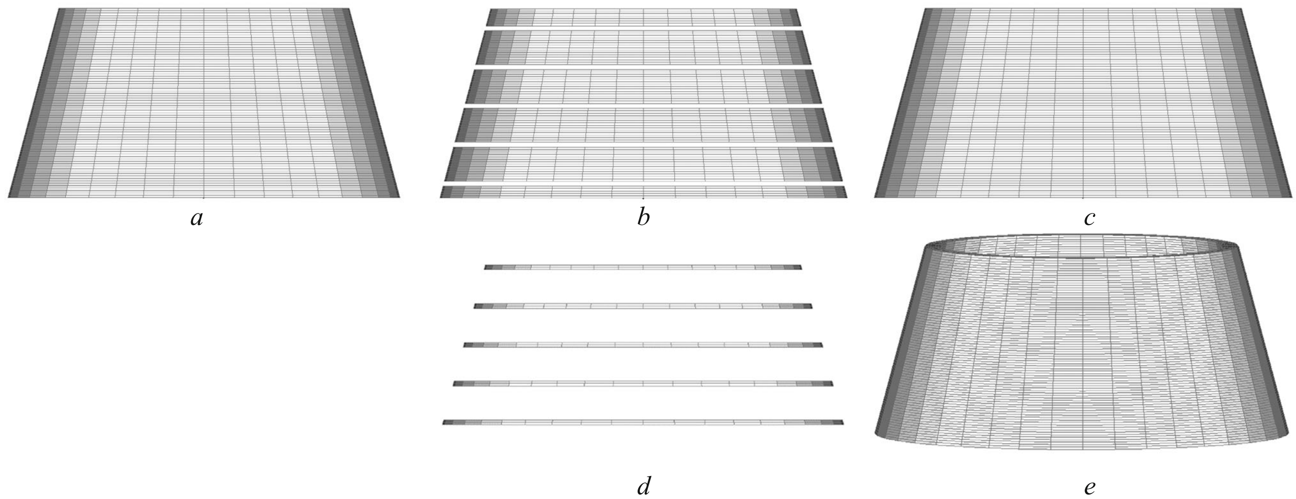

Fig. 1

In the cases of the presence of lightweight core, its characteristics are $E_{1,2} / E_t = 50 E_{1,2} / E_t = 500, \rho_t = 25$ kg/m^3, $\nu_t =$ 0.33.

The discrete reinforcement ribs are located at the points $s_j = [6 + (k-1)16]\Delta s,\ k = \overline{1,5},\ \Delta s = (s_N - s_0)/80,\ (s_N - s_0) =$ 0.39 m.

The initial–boundary-value problem (1.16), (2.1)–(2.3) is solved using the finite-element method. The finite-element shell model relates the potential strain energy and the potential of the applied forces:

$$\Pi = E - W, \tag{2.4}$$

where E is the potential strain energy; W is the potential of the applied forces.

After the continuous domain is partitioned into finite elements, model (2.4) takes the form

$$\Pi = \sum_{e=1}^{E} (E^{(e)} - W^{(e)}) = \sum_{e=1}^{E} \pi^{(e)}. \tag{2.5}$$

The global stiffness matrix and the global vector column in the matrix equation

$$[K]\{U\} = \{F\} \tag{2.6}$$

correspond to the relations

$$[K] = \sum_{e=1}^{E} [k^{(e)}],$$

$$\{F\} = -\sum_{e=1}^{E} \{f^{(e)}\}. \tag{2.7}$$

We have analyzed the dynamic stress–strain state of the symmetric conical sandwich shell. The models are based on a three-dimensional finite element that ensures the accuracy and reliability of the results [13].

Figure 1 shows the finite-element model of the sandwich conical shell with discrete symmetric lightweight core reinforced with ribs. The model has the following components: outer load-bearing layer (a), inner load-bearing layer (b); lightweight core (c); reinforcement ribs (d), sandwich shell (e). The finite-element model with a generatrix length of 0.39 m and a cone angle of 15° has 15,600 spatial finite elements and 18,960 nodes.

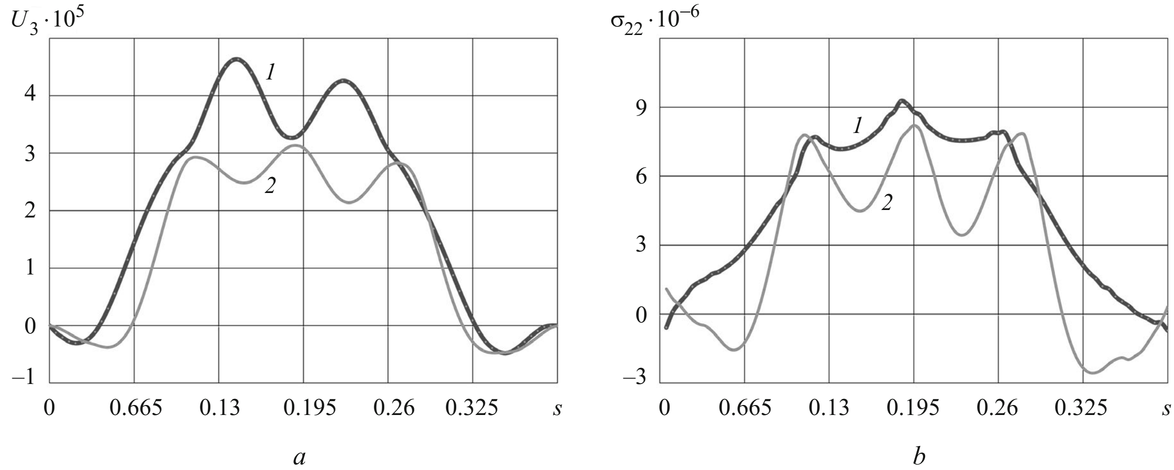

Fig. 2

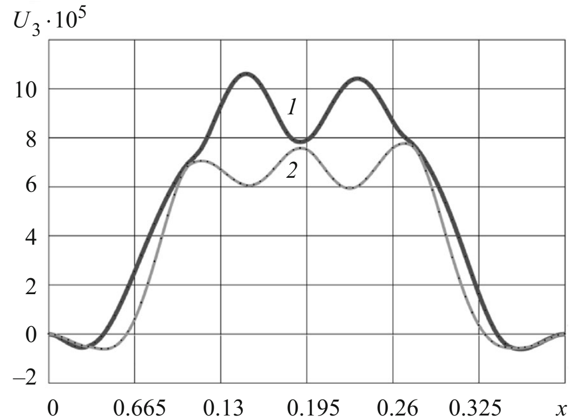

Fig. 3

The numerical results obtained allow us to analyze the stress–strain state of sandwich conical elastic shells at any instant (the computation time interval being $0 \le t \le 40T$). For example, Fig. 2*a* demonstrates how the normal deflection u_3 of the mid-surfaces of the load-bearing layers depend on the space coordinate *s*. Hereafter, curve *1* corresponds to u_3^1 of the inner shell, and curve *2* to u_3^2 of the outer shell at $t = 3.15T$ (the time the u_3 is maximum). The lightweight core is absent. The points at which curves *1* and *2* intersect indicate the position of the ribs. These plots allow visual evaluation the influence of the conicity of the shell on the antisymmetry of the distribution of u_3 along the *s*-coordinate. The first natural frequency of the shell is equal to 1602 Hz.

The results obtained are in a good agreement with those in [17].

To validate the software used, we used $\alpha = 0$ and $s = x$. The equation was derived for a cylinder of radius R_0 and length $L = S_N = 0.39$ m. The dynamic processes were studied on the time interval $0 \le t \le 40T$.

Figure 3 shows the dependence of the normal deflections u_3^1 and u_3^2 of the bearing layers in a cylindrical shell on the coordinate *x* at $t = 3.15T$ (the time the u_3 is maximum). It can be seen that the deflection u_3 for the cylindrical sandwich shell is symmetric about the central cross-section. This fact is also indicative of the reliability of the results obtained for the sandwich conical shell with the finite-element method. These results are also in a good agreement with the results obtained in [18] using the finite-difference method. The first natural frequency of the cylindrical sandwich structure is equal to 1533 Hz.

Figure 2*b* shows how the normal stress σ_{22} depends on the coordinate *s* in the sandwich conical shell. Hereafter curve *1* corresponds to σ_{22}^1 in the inner conical shell, and curve *2* to σ_{22}^2 in the outer conical shell at $t = 3.15T$ (the time σ_{22} is maximum). The lightweight core is absent. The first natural frequency of the shell is equal to 1602 Hz.

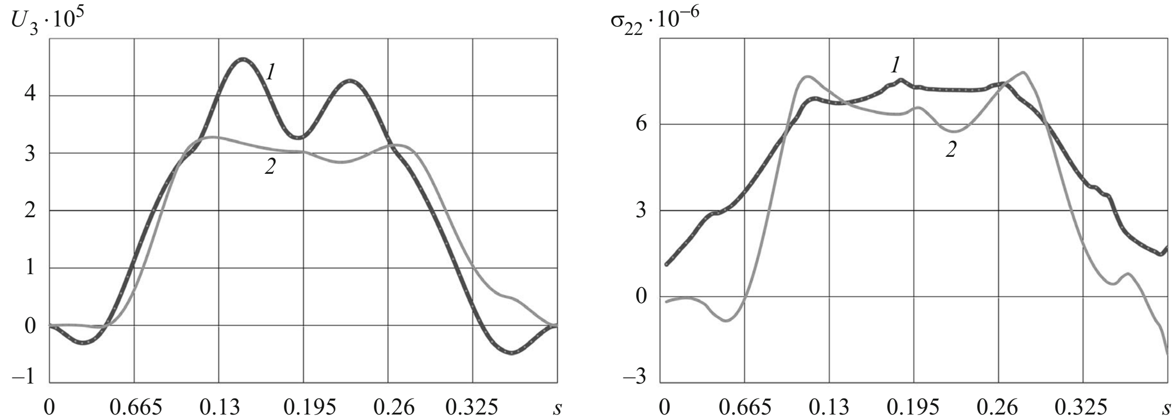

a *b*

Fig. 4

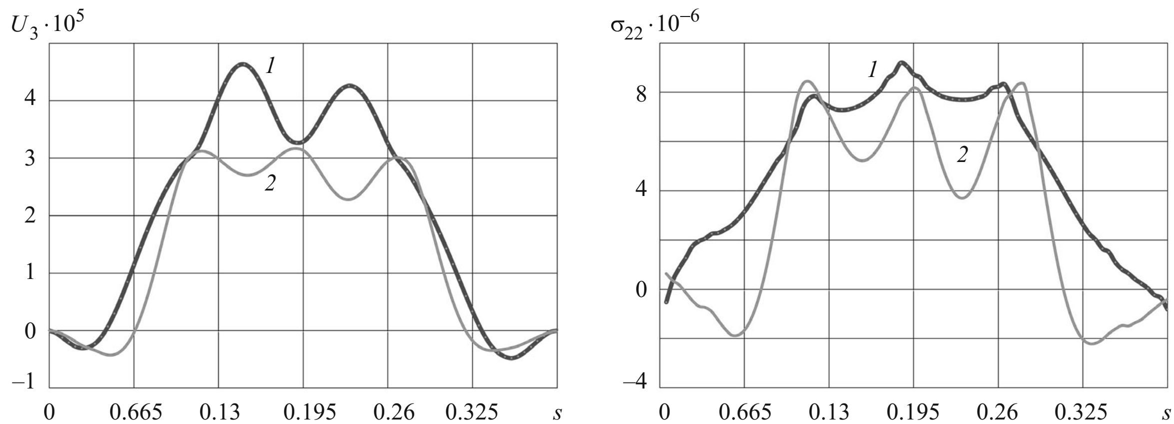

a *b*

Fig. 5

Let us analyze the influence of the lightweight core located between the load-bearing layers and the discrete symmetrical ribs of the shell. The physical and mechanical parameters of the lightweight core (foamed plastic) are: $E_{1,2} / E_t = 50, E_{1,2} / E_t = 500, \rho_t = 25$ kg/m^3, $\nu_t = 0.33$.

Figure 4*a* demonstrates the dependence of the normal deflections u_3^1 and u_3^2 of the load-bearing layers on the longitudinal coordinate *s* at $t = 2.25T$ (the time the u_3 is maximum). The ratio of the elastic moduli of the load-bearing layers and the lightweight core $E_{1,2} / E_t = 50$. The points at which curves *1* and *2* intersect indicate the position of the ribs. The curves allow visual evaluation of the influence of the conicity of the shell on the antisymmetry of distribution of u_3 along the *s*-coordinate. The first natural frequency of the shell is equal to 1774 Hz.

Figure 4*b* shows the dependencies of the normal stresses σ_{22}^1 and σ_{22}^2 in the mid-surfaces of the load-bearing layers on the coordinate *s* for $E_{1,2} / E_t = 50$ at $t = 2.25T$ (the time σ_{22} is maximum). The first natural frequency of the shell is equal to 1774 Hz.

Figure 5*a* shows the dependence of the normal deflections u_3^1 and u_3^2 of the mid-surfaces of the load-bearing layers for $E_{1,2} / E_t = 500$ on the coordinate *s* at $t = 3.0T$ (the time the u_3 is maximum). The points at which curves *1* and *2* intersect indicate the position of the ribs. The curves allow visual evaluation of the influence of the conicity of the shell on the antisymmetry of the distribution of u_3 along the space coordinate. The first natural frequency of the shell is equal to 1620 Hz.

Figure 5*b* shows the dependence of the normal stresses σ_{22}^1 and σ_{22}^2 in the mid-surfaces of the load-bearing layers for $E_{1,2} / E_t = 500$ on the coordinate *s* at $t = 3.0T$ (the time the σ_{22} is maximum). The first natural frequency of the shell is equal to 1620 Hz.

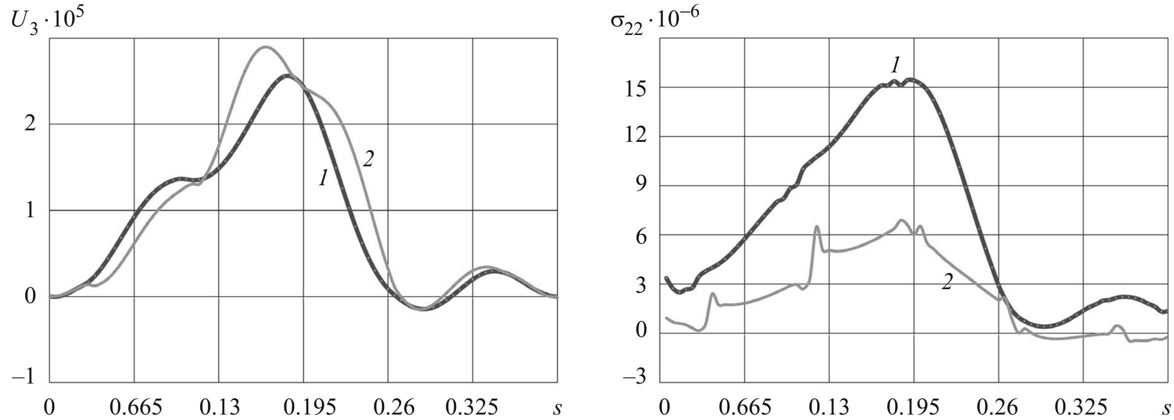

a *b*

Fig. 6

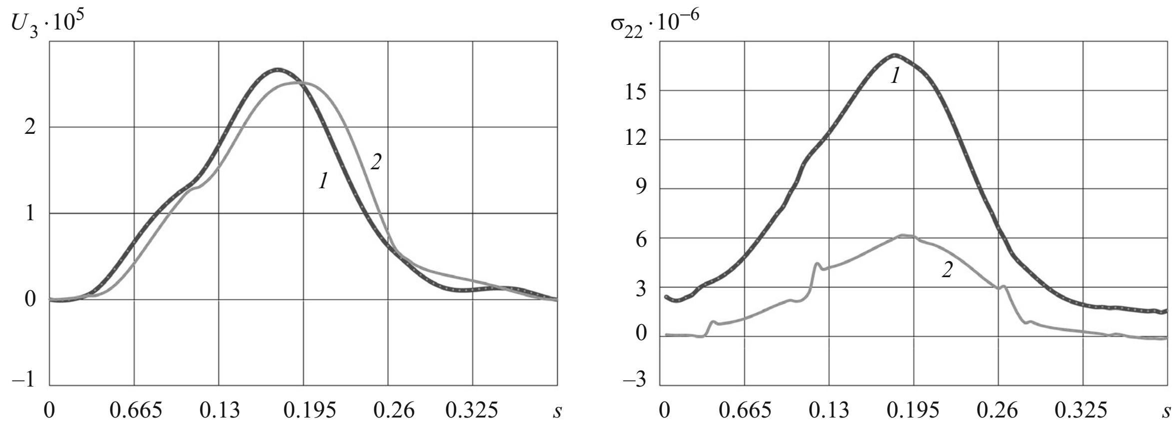

a *b*

Fig. 7

Let us now discuss the results on the influence of the cone angle $\alpha = \pi / 6 = 30°$ on the dynamic behavior of symmetric sandwich shells with discretely symmetric lightweight core reinforced with ribs. All the other dimensions and physical and mechanical parameters as well as the type of loading remain the same.

The finite-element model of the shell with a generatrix length of 0.39 m and a cone angle of 30° contains 33,696 spatial finite elements and 39,816 nodes. Using the spatial finite element ensures the requirec accuracy and reliability of the results [15]. The numerical results obtained allow us to analyze the stress–strain state of the conical elastic sandwich shell at any instant (the computation time interval being $0 \le t \le 40T$).

Figure 6*a* shows the dependence of the normal deflection u_3 of the mid-surfaces of the load-bearing layers on the coordinate *s*. Here the notation is same as for shells with a cone angle of 15°. The deflection u_3 peaks at $t = 6.95T$. The lightweight core is absent. The points at which curves *1* and *2* intersect indicate the posiiton of the ribs. The curves allow visual evaluation of the influence of the conicity of the shell on the antisymmetry of distribution of u_3 along the coordinate *s*. The first natural frequency of the shell is equal to 1514 Hz.

Figure 6*b* demonstrates the dependence of the maximum normal stresses σ_{22}^1 and σ_{22}^2 in the mid-surfaces of the load-bearing layers of the shell without core on the coordinate *s* at $t = 6.95T$. The first natural frequency of the shell is equal to 1514 Hz.

Figure 7*a* shows the dependence of the maximum normal deflection u_3 of the mid-surfaces of the load-bearing layers on the coordinate *s* for $E_{1,2} / E_t = 50$ at $t = 6.45T$. The points at which curves *1* and *2* intersect indicate the position of the ribs. The curves allow visual evaluation of the influence of conicity on the anti-symmetry of the distribution of u_3 along the coordinate *s*. The first natural frequency of the shell is equal to 1655 Hz.

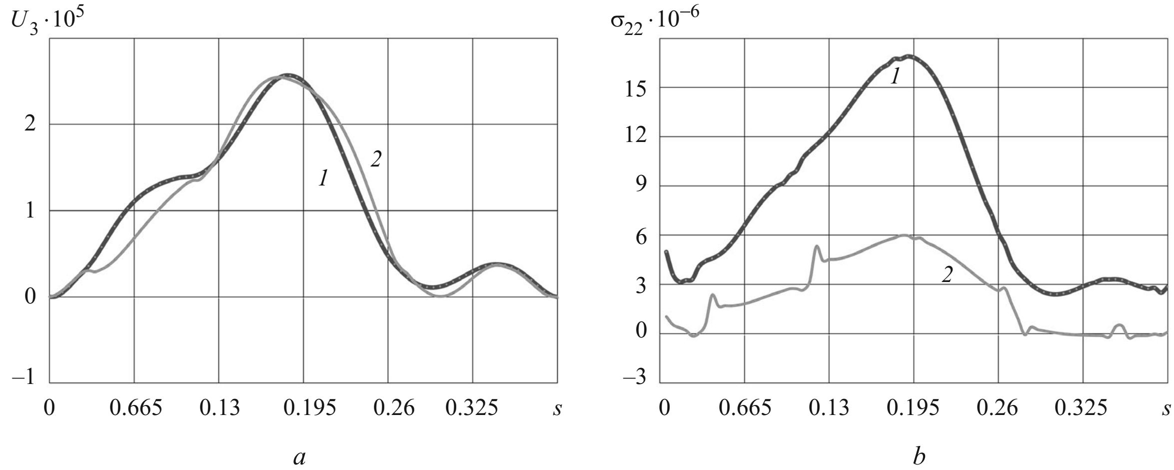

Fig. 8

Figure 7*b* demonstrates the dependence of the maximum normal stress σ_{22} in the mid-surfaces of the load-bearing layers on the coordinate *s* for $E_{1,2} / E_t = 50$ at $t = 6.45T$. The curves allow visual evaluation of the influence of conicity on the anti-symmetry of the distribution of σ_{22} along the coordinate *s*. The first natural frequency of the shell is equal to 1655 Hz.

Figure 8*a* shows the dependence of the maximum normal deflection u_3 of the mid-surfaces of the load-bearing layers on the coordinate *s* for $E_{1,2} / E_t = 500$ at $t = 6.60T$. The points at which curves *1* and *2* intersect indicate the position of the ribs. The curves allow visual evaluation of the influence of conicity on the anti-symmetry of the distribution of u_3 along the coordinate *s*. The first natural frequency of the shell is equal to 1532 Hz.

Figure 8*b* shows the dependence of the maximum normal stress σ_{22} in the mid-surfaces of the load-bearing layers on the coordinate *s* for $E_{1,2} / E_t = 500$ at $t = 6.60T$. The curves allow visual evaluation of conicity on the anti-symmetry of the distribution of σ_{22} along the coordinate *s*. The first natural frequency of the shell is equal to 1532 Hz.

3. Nonstationary Forced Vibrations of Asymmetric Conical Sandwich Shells with a Discretely Symmetric Lightweight Core Reinforced with Ribs. The dynamics and statics of layered shells was studied in many works, including [1, 2, 4, 5, 20–22], where a great number of fundamental problems were solved using analytical and approximate methods. The vibration behavior of asymmetric sandwich shells with a lightweight core was analyzed in [13]. In what follows, we will study, using the finite-element method, the non-stationary forced vibrations of non-symmetric conical sandwich shells with a discretely symmetric lightweight core reinforced with ribs. The load-bearing layers are made of dissimilar materials. In this case, Eqs. (1.16) are decomposed due to not only the presence of discontinuous coefficients in the last three equations but also the dissimilarity of the layer materials. The finite-element model of a shell with a generatrix length of 0.39 m and a cone angle of 15°, contains 15,600 spatial finite elements and 18,960 nodes (Fig. 1).

Input data:

$$E_1^1 = 2 \cdot 10^{11} \text{ Pa}, \quad E_1^2 = E_j = 7 \cdot 10^{10} \text{ Pa}, \quad \rho_1^1 = 7.8 \cdot 10^3 \text{ kg/m}^3, \quad \rho_2^1 = \rho_j = 2.7 \cdot 10^3 \text{ kg/m}^3,$$

$$R_0 = 0.3 \text{ m}, \quad R_0 / h_1 = 30, \quad h_1 = h_2 = h_j = 0.01 \text{ m}, \quad H_j = 2h_1, \quad \alpha = \pi / 12 = 15°, \quad F_j = 2 \cdot 10^{-4} \text{ m}^2.$$

The non-stationary impulsive loading is defined by (2.3). The inside layer is made of steel, while the outside layer is made of AMG-6 alloy; the thickness of the foam plastic core is 0.02 m, the ratio of the moduli of the load-bearing layers and the filler is $(E_1 + E_2) / 2E_t = 50$. The reinforcement ribs are located at the points $s_j = [6 + (k-1)16]\Delta s$, $k = \overline{1,5}$, $\Delta s = (s_N - s_0) / 80$, $(s_N - s_0) = 0.39$ m.

The numerical results obtained allow us to analyze the stress–strain state of asymmetric sandwich conical elastic shells at any instant (the computation period being $0 \le t \le 40T$).

Figure 9*a* demonstrates the dependence of the normal deflection u_3 of the mid-surfaces of the load-bearing layers on the coordinate *s* at $t = 3.1T$ (the time the u_3 is maximum). The core is absent. The points at which curves *1* and *2* intersect indicate the

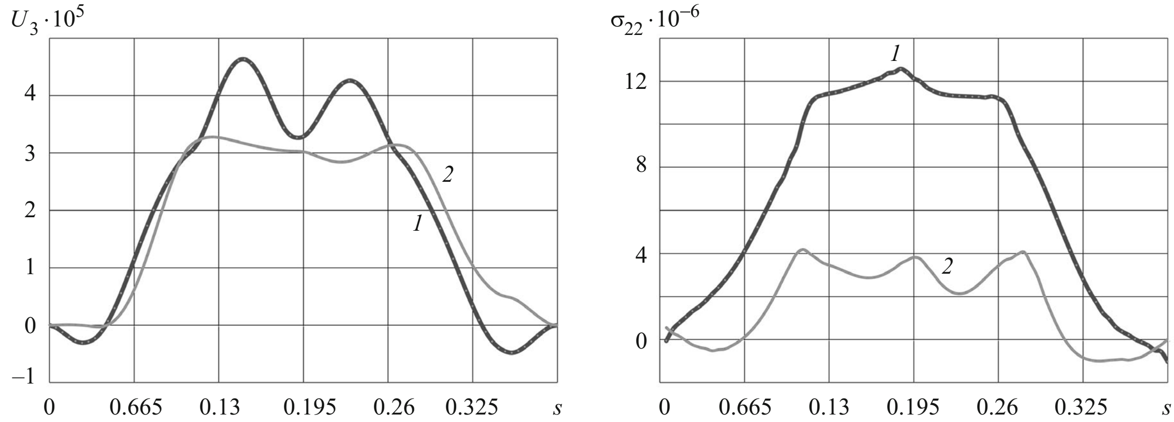

a *b*

Fig. 9

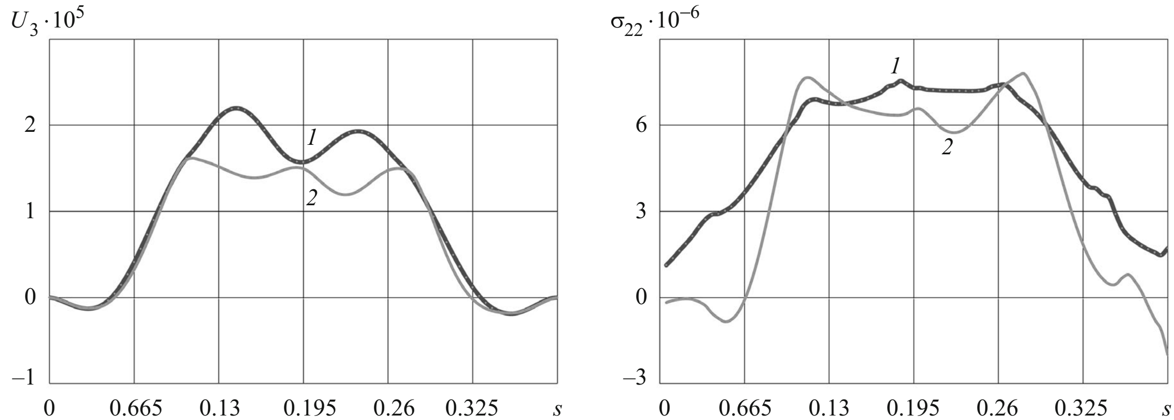

a *b*

Fig. 10

position of the ribs. These plots allow visual evaluation of the influence the conicity of the shell on the anti-symmetry of the distribution of u_3 along the spatial coordinate. The first natural frequency of the conical shell is equal to 1559 Hz.

Figure 9*b* shows the dependence of the normal stress σ_{22} in the mid-surfaces of the load-bearing layers on the coordinate *s* at $t = 3.1T$ (the time the σ_{22} is maximum). The first natural frequency of the conical shell is equal to 1559 Hz. The core is absent. The points at which curves *1* and *2* intersect indicate the position of the ribs. These plots allow visual evaluation of the influence of the conicity of the shell on the anti-symmetry of distribution of σ_{22} along the spatial coordinate.

Figure 10*a* demonstrates the dependence of the normal deflection u_3 of the mid-surfaces of the load-bearing layers on the coordinate *s* at $t = 2.45T$ (the time the u_3 is maximum). The ratio of elastic moduli $(E_1 + E_2)/2E_t = 50$. The points at which curves *1* and *2* intersect indicate the position of the ribs. These plots allow visual evaluation of the influence of conicity on the anti-symmetry of the distribution of u_3 along the spatial coordinate. The first natural frequency of the conical shell is equal to 1746 Hz.

Figure 10*b* shows the dependence of the normal stress σ_{22} in the mid-surfaces of the load-bearing layers on the coordinate *s* at $t = 2.45T$ (the time the σ_{22} is maximum). The ratio of the elastic moduli $(E_1 + E_2)/2E_t = 50$. These plots allow visual evaluation of the influence of conicity on the anti-symmetry of the distribution of σ_{22} along the spatial coordinate. The first natural frequency of the conical shell is equal to 1746 Hz.

Conclusions. In solving the problem for sandwich conical shells, we have used the independent Timoshenko static and kinematic hypotheses for each layer. This has increased the order of the governing equations of vibrations of shells with a discretely symmetric lightweight core reinforced with ribs, but made it possible to study in more detail the dynamic processes in these shells. Using the finite-element method, we have demonstrated that the geometric, physical, and mechanical parameters of the shell layers have strong quantitative and qualitative effects on the vibrations of conical sandwich shells. In a symmetric conical shell without foam plastic core, as the cone angle increases by 15°, the deflection u_3^1 decreases by 74%, the circumferential stresses increase by 64%, and the first natural frequency decreases by 6%. This indicates that the bending stresses make a major contribution to the stress–strain state of the conical shell with a great cone angle, and the shell vibrates slower. The first natural frequency increases by 11% for the symmetric conical shell with a cone angle of 15° and inside layer made of foam plastic with $E_{1,2} / E_t = 50$ and by 14% for the asymmetric conical structure with foam plastic $E_{1,2} / E_t = 50$. If the inside load-bearing layers of asymmetric conical shells are made of steel, the first natural frequencies decrease due to the increase in their weight.

REFERENCES

1. A. E. Babaev and V. D. Kubenko, *Dynamics of Structural Elements*, Vol. 9 of the 12-volume series *Mechanics of Composite Materials* [in Russian], A.S.K., Kyiv (1999).
2. Ya. M. Grigorenko, *Isotropic and Anisotropic Layered Shells of Revolution of Variable Stiffness* [in Russian], Naukova Dumka, Kyiv (1973).
3. T. A. Emel'yanova, "Governing equation of free vibrations of a sandwich cylindrical shell reinforced with stiffening ribs," *Visn. Kherson. Univ.*, **2**, No. 57, 11–16 (2016).
4. P. Z. Lugovoi and V. F. Meish, "Numerical simulation of the dynamic behavior and strength analysis of multilayer shells under impulsive loading," *Strength of Materials*, **32**, No. 4, 368–375 (2000).
5. P. Z. Lugovoi, Yu. V. Skosarenko, and S. P. Orlenko, "Application of the spline-collocation method to solve static and dynamic problems for inhomogeneous cylindrical shells," *Dop. NAN Ukrainy*, No. 8, 25–33 (2019).
6. P. Z. Lugovoi and S. P. Orlenko, "Statement and solution of dynamic problems of the theory of conical sandwich shells with discrete ribbed core," in: *Proc. 17th Conf. on Improvement of Power Plants by Methods of Mathematical and Physical Simulation* [in Ukarinian], Kharkiv, October 7–11 (2019), p. 14.
7. P. Z. Lugovoi, O. P. Shugailo, S. P. Orlenko, and V. M. Demenkov, "Vibrations of heat-insulating three-layer cylindrical pipes under operating loads," *Yadern. Radiats. Besopasn.*, No. 3, 55–61 (2020).
8. V. F. Meish and S. E. Shtantsel, "Analysis of non-stationary forced vibrations of sandwich conical shells with inhomogeneous core," in: Collection of Research Papers of National Transport. Univ. "System Control Methods, Technology and Industrial Engineering, Repair and Vehicle Operation," **12**, 417–420 (2001).
9. S. P. Orlenko, "Dynamics of sandwich conical shells with reinforcement and masses," in: *Proc. 10th Conf. on Mathematical Problems of the Mechanics of Inhomogeneous Structures* [in Ukrainians], Lviv (2019), pp. 72–73.
10. S. P. Orlenko, "Numerical simulation of the vibrations of a sandwich conical shell with a discrete symmetric inhomogeneous core," *Dop. NAN Ukrainy*, No. 8, 35–42 (2020).
11. S. P. Orlenko, "Influence of the nonsymmetry of sandwich cylindrical shells with a lightweight core on their stress–strain state under non-stationary loading," *Probl. Obchysl. Mekh. Mitsn. Konstr.*, No. 31, 42–52 (2020).
12. V. G. Piskunov and A. O. Rasskazov, "Development of the theory of layered plates and shells," in *Advances in Mechanics* [in Russian], Vol. 3, A.S.K., Kyiv (2007), pp. 141–175.
13. S. P. Rychkov, *Modeling of Structures in the Femap Environment with NX Nastran* [in Russian], DMK Press, Moscow (2013).
14. S. P. Timoshenko and S. Woinowsky-Krieger, *Theory of Plates and Shells*, McGraw-Hill, New York (1966).
15. Y. Frostig and O. T. Thomsen, "Higher-order free vibration of sandwich panels with a flexible core," *Int. J. Solids Struct.*, **41**, 1697–1724 (2004).
16. M. M. Kheirikhah, S. M. R. Khalili, and K. Malekzadeh Fard, "Biaxial buckling analysis of soft-core composite sandwich plates using improved high-order theory," *European J. Mechanics A/Solids*, **31**, 54–66 (2011).
17. P. Z. Lugovoi, V. F. Meish, and S. E. Shtantsel, "Forced nonstationary vibrations of a sandwich cylindrical shell with cross-ribbed core," *Int. Appl. Mech.*, **41**, No. 2, 161–167 (2005).

18. P. Z. Lugovoi, Yu. V. Skosarenko, S. P. Orlenko, and O. P. Shugailo, “Application of the spline-collocation method to solve problems of statics and dynamics for multilayer cylindrical shells with design and manufacturing features,” *Int. Appl. Mech.*, **55**, No. 5, 524–533 (2019).
19. P. Z. Lugovoi, V. F. Meish, Yu. A. Meish, and S. P. Orlenko, “Dynamic design of compound shell structures of revolution under nonstationary loads,” *Int. Appl. Mech.*, **56**, No. 1, 22–32 (2020).
20. P. Z. Lugovoi, V. F. Meish, and S. P. Orlenko, “Numerical simulation of the dynamics of spherical sandwich shells reinforced with discrete ribs under a shockwave,” *Int. Appl. Mech.*, **57**, No. 5, 590–598 (2021).
21. P. Z. Lugovyi, V. V. Gaidaichuk, V. V. Skosarenko, and K. E. Kotenko, “Stress–strain state of thee-layer cylindrical shells with reinforced light core under nonstationary loading,” *Int. Appl. Mech.*, **57**, No. 4, 394–505 (2021).
22. P. Z. Lugovyi and S. P. Orlenko, “Effect of the asymmetry of cylindrical sandwich shells on their stress-strain state under non-stationary loading,” *Int. Appl. Mech.*, **57**, No. 5, 543–553 (2021).
23. M. Surianinov, T. Yemelianova, and D. Lazarieva, “Investigation of free vibrations of three-layered cylindrical shell supported by transverse ribs,” *Int. J. Eng. Technol.*, **11**, No. 1, 61–66 (2019).